Pis'ma v ZhETF, vol. 94, iss. 5, pp. 377 – 382

Effect of spontaneously generated coherence on left-handedness in a degeneracy atomic system

S.-C. Zhao[1)]

Physics department, Kunming University of Science and Technology, Kunming, 650093, China

Submitted 4 May 2011

Resubmitted 18 August 2011

A theoretical investigation is carried out into the effect of spontaneously generated coherence (SGC) on the left-handedness in a four-level Y-type atomic system with two highest nearly degenerate lying levels. It is found, with the spontaneously generated coherence intensity enhancing, the atomic system gradually displays left-handedness with simultaneous negative permittivity and permeability. And the refractive index enhances with the increasing intensity of SGC. However, the absorption is suppressed by the SGC effect when the SGC has a large intensity. When the probe field is near-resonant coupled to the atomic system, the appearance of SGC doesn't always change the permeability from positive to negative and allow for left-handed behavior, unless the SGC reaches a large intensity.

I. Introduction. Quantum interference in quantum optics occurs when there are two or more identical channels in a transition. The simplest example is classic Fano interference [1,2] from a continuum of upper states to a ground state. Another intriguing quantum effect is the interference of two decay channels with nonorthogonal electric-dipole transition matrix elements. This is named as "spontaneously generated coherence" (SGC) [3,4] which was first suggested by Agarwal [4] who showed that the spontaneous emission from a degenerate V-type three-level atom is sensitive to the mutual orientation of the atomic dipole moments. If they are parallel a suppression of spontaneous emission can appear and a part of the population can be trapped in the excited levels. SGC is one of the two mechanisms of generating quantum coherence applied by incoherent processes, i.e., spontaneous emission [5], and the other one is by coherent fields, such as laser fields [6–9] or microwave fields [10]. Here we are particularly interested in the former case and impressive efforts have been made to investigate it in the last few decades[11–20]. SGC requires two close-lying levels be nearly degenerate and the atomic dipole moments be nonorthogonal when the atom is placed in free space. And it is responsible for many important physical phenomena, which are potentially applied in lasing without population inversion [11], coherent population trapping (CPT) [12], group velocity reduction [13], ultrafast all-optical switching [14], transparent high-index materials [21], high-precision spectroscopy and magnetometer [22], modified quantum beats [23], dark-state polaritons [24], quantum information and computing [25], etc. In order to observe the phenomena based on SGC, a few methods have been proposed to simulate this intriguing effect. SGC can be simulated by a dc field [26], a microwave field [27], or a laser field [28–30]. Very recently, there is experimental evidence that SGC plays a role in charged GaAs quantum dots [31], which have been proposed as elements in qu antum-information networks. All the interesting features due to SGC could have useful applications in laser physics and other areas of quantum optics.

Although some works [32,33] for the realization of negative refraction have been done, the dependence of SGC effect on the left-handedness has never been investigated to our best knowledge. Materials with left-handedness (medium having negative permittivity and permeability simultaneously) which originally suggested by Veselago [34], promise many surprising and even counterintuitive electromagnetical and optical effects such as the reversals of both Doppler shift and Cerenkov radiation [34], negative Goos–Häanchen shift [35], amplification of evanescent waves [36], sub-wavelength focusing [37] and so on. Up to now, several interesting approaches have been proposed to realize LHM, such as the method of artificial composite metamaterials [38–40], the method of specific photonic crystal structures [41,42], the method of chiral materials [43,44], and the method of photonic resonant media [45–48]. In this paper, we investigate the effects of SGC on left-handedness in a four-level Y-type atomic system. When the two highest-lying levels of atomic system are nearly degenerate and coupled by the same vacuum radiation field to the intermediate state, the system can create SGC due to the quantum interference between the two spontaneous decay channels.

[1)] e-mail: zscnum1@126.com.

And Our paper is organized as follows. In Sec. II we describe the model and present the density-matrix equations of motion for the system. In Sec. III we discuss the effects of SGC on the left-handedness. The dependence of simultaneous negative permittivity and permeability with SGC is discussed here. In Sec. IV, the conclusion is presented.

II. Theoretical analysis. We consider a four-level Y-type atomic system as shown in Fig. 1. A resonant

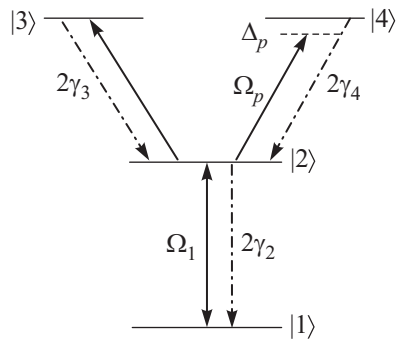

Fig. 1. Schematic representation of the relevant atomic energy levels

coupling field Ω_1 drives the transition between levels $|1\rangle$ and $|2\rangle$ while a probe field Ω_p is applied to the transition $|2\rangle$ and $|4\rangle$. Its electric (E) and magnetic (B) components of the probe field couple state $|2\rangle$ to state $|4\rangle$ by an electric dipole transition, and to state $|3\rangle$ by a magnetic dipole transition. The parities in this system are $|2\rangle$ even, $|3\rangle$ even, $|4\rangle$ odd or vice versa. $2\gamma_3$ and $2\gamma_4$ are the spontaneous decay rates from levels $|3\rangle$ and $|4\rangle$ to level $|2\rangle$, respectively, and $2\gamma_2$ corresponds to the decay rate from $|2\rangle$ to $|1\rangle$. In the interaction picture the density-matrix equations of motion in the rotating-wave approximations can be written as

$$\dot{\rho_{11}} = 2\gamma_2\rho_{22} + i\Omega_1(\rho_{21} - \rho_{12}), \tag{1}$$

$$\dot{\rho_{33}} = 2\gamma_3\rho_{33} - p\sqrt{\gamma_3\gamma_4}(\rho_{34} + \rho_{43}), \tag{2}$$

$$\dot{\rho_{44}} = -2\gamma_4\rho_{44} - p\sqrt{\gamma_3\gamma_4}(\rho_{34}+\rho_{43}) + i\Omega_p(\rho_{24}-\rho_{42}), \tag{3}$$

$$\dot{\rho_{12}} = -\gamma_2\rho_{12} + i\Omega_1(\rho_{22} - \rho_{11}) - i\Omega_p\rho_{14}, \tag{4}$$

$$\dot{\rho_{13}} = -\gamma_3\rho_{13} + i\Omega_1\rho_{23} - p\sqrt{\gamma_3\gamma_4}\rho_{14}, \tag{5}$$

$$\dot{\rho_{14}} = -(\gamma_4 - i\Delta_p)\rho_{14} - p\sqrt{\gamma_3\gamma_4}\rho_{13} + i\Omega_1\rho_{24} - i\Omega_p\rho_{12}, \tag{6}$$

$$\dot{\rho_{23}} = -(\gamma_2+\gamma_3)\rho_{23} + i\Omega_1\rho_{13} + i\Omega_p\rho_{43} - p\sqrt{\gamma_3\gamma_4}\rho_{24}, \tag{7}$$

$$\dot{\rho_{24}} = -(\gamma_2 + \gamma_4 - i\Delta_p)\rho_{24} + i\Omega_p(\rho_{44} - \rho_{22}) + i\Omega_1\rho_{14} - p\sqrt{\gamma_3\gamma_4}\rho_{23}, \tag{8}$$

$$\dot{\rho_{34}} = -(\gamma_3+\gamma_4-i\Delta_p)\rho_{34} - i\Omega_p\rho_{32} - p\sqrt{\gamma_3\gamma_4}(\rho_{33}+\rho_{44}). \tag{9}$$

The above equations are constrained by $\rho_{11} + \rho_{22} + \rho_{33} + \rho_{44} = 1$ and $\rho_{ij} = \rho^*_{ji}\Delta_p = \omega_{24} - \omega_p$ means the detuning of the probe field from the optical transition. The terms with $p\sqrt{\gamma_3\gamma_4}$ represent the quantum interference resulting from the cross coupling between spontaneous emission paths $|3\rangle - |2\rangle$ and $|4\rangle - |2\rangle$.

The parameter p denotes the alignment of the two dipole moments. If the two dipole moments are orthogonal to each other, i.e., $p = 0$, the SGC effect disappears. While for the parallel or antiparallel case we have $p = \pm 1$, the interference between the spontaneous emissions and the SGC-effect reach the maximum. So we can depict dynamic intensity of the SGC-effect by parameter p. With the restriction that each field acts only on one transition, the Rabi frequencies Ω_1 and Ω_P are represented by $\Omega_{1(P)} = \Omega^0_{1(P)}\sqrt{1-p^2}$. It should be noted that only for small energy spacing between the two highest-lying levels are significant; otherwise the oscillatory terms will average out to zero and thereby the SGC-effect vanishes [49–51].

In the following, we will discuss the electric and magnetic responses of the medium to the probe field. It should be noted that here the atoms are assumed to be nearly stationary (e.g., at a low temperature) and hence any Doppler shift is neglected. When discussing how the detailed properties of the atomic transitions between the levels are related to the electric and magnetic sus-ceptibilities, one must make a distinction between macroscopic fields and the microscopic local fields acting upon the atoms in the vapor. In a dilute vapor, there is little difference between the macroscopic fields and the local fields that act on any atoms (molecules or group of molecules) [52]. But in dense media with closely packed atoms (molecules), the polarization of neighboring atoms (molecules) gives rise to an internal field at any given atom in addition to the average macroscopic field, so that the total fields at the atom are different from the macroscopic fields [52]. In order to achieve the negative permittivity and per-meability, here the chosen vapor with atomic concentration $N = 5 \cdot 10^{24} m^{-3}$ should be dense, so that one should consider the local field effect, which results from the dipole-dipole interaction between neighboring atoms. In what follows we first obtain the atomic electric and magnetic polarization, and then consider the local field correction to the electric and magnetic suscep-tibilities (and hence to the permittivity and permeability) of the coherent vapor medium. With the formula of the atomic electric polarizations $\gamma_e = 2d_{42}\rho_{24}/\epsilon_0 E_p$, where $E_p = \hbar\Omega_p/d_{42}$ one can arrive at

$$\gamma_e = \frac{2d^2_{24}\rho_{24}}{\epsilon_0\hbar\Omega_p}. \tag{10}$$

In the similar fashion, by using the formulae of the atomic magnetic polarizations $\gamma_m = 2\mu_0\mu_{23}\rho_{32}/B_p$ [52], and the relation of between the microscopic local electric and magnetic fields $E_p/B_p = c$ we can obtain the explicit expression for the atomic magnetic polarizability. Where μ_0 is the permeability of vacuum, c is the speed of light in vacuum. Then, we have obtained the microscopic physical quantities γ_e and γ_m. Thus, the coherence ρ_{32} drives a magnetic dipole, while the coherence ρ_{24} drives an electric dipole. However, what we are interested in is the macroscopic physical quantities such as the electric and magnetic susceptibilities which are the electric permittivity and magnetic permeability. The electric and magnetic Clausius–Mossotti relations can reveal the connection between the macroscopic and microscopic quantities. According to the Clausius–Mossotti relation [53], one can obtain the electric susceptibility of the atomic vapor medium

$$\chi_e = N\gamma_e(1 - N\gamma_e/3)^{-1}. \tag{11}$$

The relative electric permittivity of the atomic medium reads $\varepsilon_r = 1 + \chi_e$. In the meanwhile, the magnetic Clausius–Mossotti [53]

$$\gamma_m = \frac{1}{N}\frac{\mu_r - 1}{2/3 + \mu_r/3} \tag{12}$$

shows the connection between the macroscopic magnetic permeability μ_r and the microscopic magnetic polarizations γ_m. It follows that the relative magnetic permeability of the atomic vapor medium is

$$\mu_r = \frac{1 + (2/3)N\gamma_m}{1 + (1/3)N\gamma_m}. \tag{13}$$

Substituting the expressions of ε_r and μ_r into $n = e\sqrt{\varepsilon_r\mu_r}$ [34], we can get the refractive index of left-handed materials. In the above, we obtained the expressions for the electric permittivity, magnetic permeability and refractive index of the four-level atomic medium. In the section that follows,we will get solutions to the density-matrix equations (1) under the stead-state condition.

For simplicity, we scale all the parameters by $\gamma = 10^8$, $\Omega_1^0 = 10\gamma$, $\Omega_p^0 = 0.2\gamma$, $\gamma_2 = \gamma_3 = \gamma_4 = 0.8\gamma$ during our calculation. Analyzing the left-handed behavior in the atomic system, the plus or minus for the real part of permittivity ϵ_r and permeability μ_r is the content for considered. We show in Fig. 2 the real part of the relative electric permittivity ε_r as a function of the probe rescaled detuning Δ_p/γ. Curves of different colors corresponds to different values of p noted in the caption of Fig. 2. We noticed that the real part of relative electric permittivity er always remains negative in the range

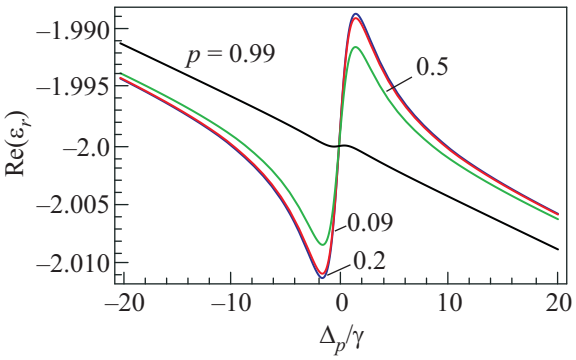

Fig. 2. Real parts of the permittivity as a function of the rescaled detuning parameter Δ_p/γ with: $\Omega_1^0 = 10\gamma$, $\Omega_p^0 = 0.2\gamma$, $\gamma_2 = \gamma_3 = \gamma_4 = 0.8\gamma$. The curves are labeled by p values

of detuning considered here while varying the value of p, and the line shape is similar in Fig. 2. The contribution of local field due to dipole-dipole interaction plays an important role in the real parts of permittivity remaining negative values, because the atomic density is assumed very high here. We also noticed that when $p = 0.99$ which means a strong interference between the two spontaneous emission channels and the SGC-effect is strongest, the fluctuation range $\mathrm{Re}\,\epsilon_r$ is the smallest near the resonant point.

In Fig. 3, the real part of magnetic permeability μ_r versus Δ_p/γ is plotted with the same parameters as

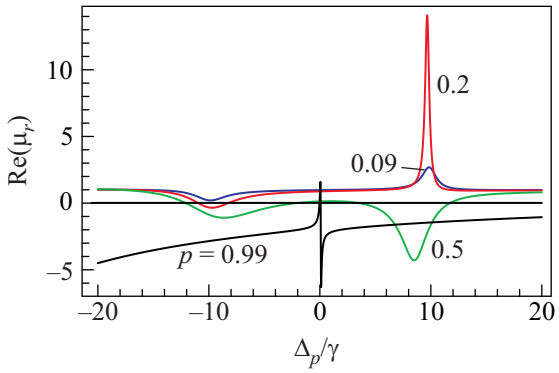

Fig. 3. Real parts of the permeability as a function of the rescaled detuning parameter Δ_p/γ. The curves are labeled by p values

used in Fig. 2. It shows that when $p = 0.09$, $\mathrm{Re}\,\mu_r$ is always positive in the detuning range. The atomic system shows no left-handed behavior with the weak SGC-effect caused by the interference between the spontaneous emission channels. Because the left-handed material (LHM), should possess negative real parts of both dielectric permittivity er and magnetic permeability μ_r over the same frequency band. The magnetic response

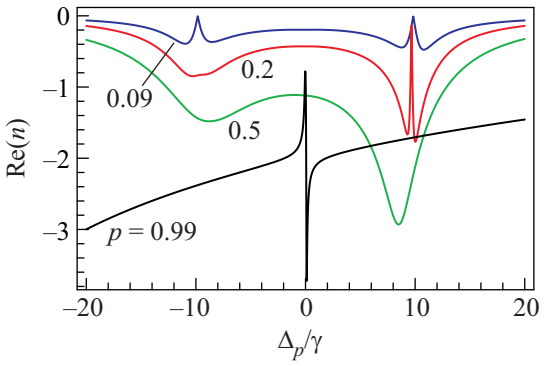

Fig. 4. Real parts of the refractive index as a function of the rescaled detuning Δ_p/γ

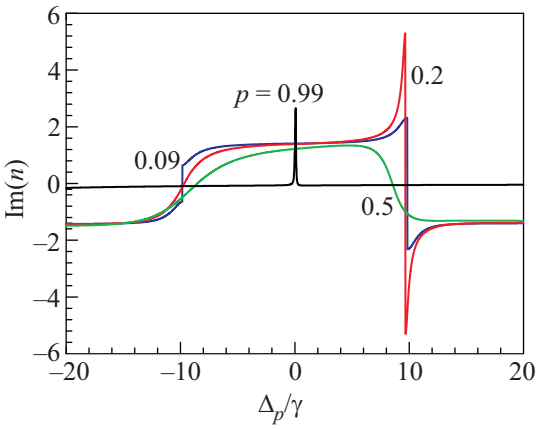

Fig. 5. Real part of the permitivity and permeability as a function of p with the probe field near-resonant coupling

of our atomic system is quite different when the SGC gets a large intensity. $\mathrm{Re}\,\mu_r$ is firstly negative value in a small frequency band near $\Delta_p = 10\gamma$ when p reaches the value of 0.2 as shown in Fig. 2. Two larger frequency ranges show that $\mathrm{Re}\,\mu_r$ is negative when $p = 0.5$. Further increasing p to the value of 0.99, the negative $\mathrm{Re}\,\mu_r$ is in all the detuning range except the resonant point. The SGC is stronger, the wider and much more frequency ranges for negative permeability. That is, the SGC-effect greatly enhances the magnetic response of a dense atomic gas so that one can realize negative refractive index. Here, we stress that the refractive index for left-handed materials is given by $n = -\sqrt{\varepsilon_r \mu_r}$, where the symbol "−" corresponds to the only case of both ε_r and μ_r having negative real parts. The enhancement of SGC results the simultaneously negative real parts for permittivity and permeability. Hence, we attribute the emergence of left-handedness to the enhancement of the SGC-effect which induced by the interference between the two spontaneous emission channels from the two highest-lying levels in the atomic system.

In Fig. 4, the refractive index is plotted for different values of the parameter p with the same parameters as used in Fig. 2. As observed in Fig. 4, the amplitude of the real parts of refractive index gradually increases as the intensifying of SGC. The maximum value of $\mathrm{Re}\,n$ are -1.7, -2.9, -3.7 when p is varied by 0.2, 0.5, 0.99, respectively. Obviously, the intensity of SGC-effect influences its peak value. The imaginary part of refractive index which depicts the atomic system absorption property is plotted on the right side of Fig. 4. Two transparency windows turn into two transparency ranges beside the resonance. The absorption is suppressed by the SGC-effect when it has a large intensity shown by Fig. 4.

Above, we discussed the left-handedness as functions of the detuning parameter Δ_p/γ. In order to get a deeper insight into the effect of SGC on left-handedness, in Fig. 5 and 6, we plot the case of the probe field near-resonantly coupling $|2\rangle$ and $|4\rangle$ ($\Delta_p = 10^{-16}\gamma$) with other parameters being the same as used in Fig. 2. And here, the characteristic parameters of left-handedness is depicted as the functions of p which will value from the orthogonality to alignment of the two dipole moments, because the conclusion of anti-alignment will be symmetric to the alignment.

In Fig. 5, we notice that the real part of the relative electric permittivity ϵ_r maintains negative value by varying p from 0 to 1. And its value reaches to -2 when $p = 1$. It shows the intensity of SGC can change the value of $\mathrm{Re}\,\epsilon_r$ but not change its sign property of plus or minus because of the local field due to dipole-dipole interaction causing by the high atomic density here. However, the line shape of $\mathrm{Re}\,\mu_r$ shows different characteristic, when p is in different value range. In the range of $[0, 0.55]$, $\mathrm{Re}\,\mu_r$ is positive. But it's negative in the range of $[0.55, 1]$. And the left-handedness will appear in the range $[0.55, 1]$ with negative permittivity and permeability simultaneously. It shows that the magnetic response of the atomic system is different under the condition of large SGC-effect. In the atomic system, the weak SGC can't cause left-handedness but the intensifying SGC can do. The refractive index is potted versus p in Fig. 6. The real part of refractive index shows the increasing of SGC-effect can bring about the negative maximum -2. However, its imaginary part illustrates the enhancement of SGC-effect can keep down the absorption, which is certainly favorable for potential experiments.

From the point of application, the atomic scheme in Fig. 1 may be realized by the Rb atom with $5S_{1/2}$, $5P_{3/2}$, $5D_{3/2}$, and $5D_{5/2}$ behaving as the $|4\rangle$, $|1\rangle$, $|2\rangle$, and $|3\rangle$ state labels, respectively. The state $5D_{3/2}$ is coupled to the state $5D_{5/2}$ by a resonant microwave field in

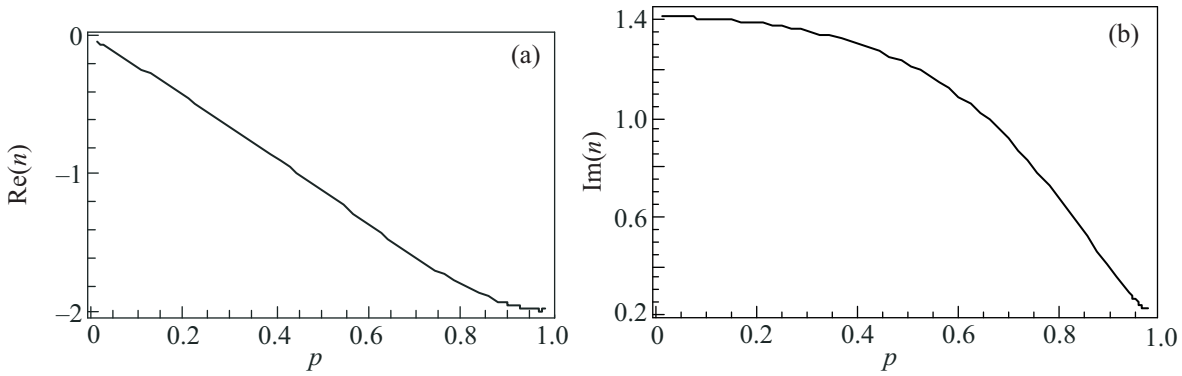

Fig. 6. Real and imaginary parts of the refractive index as a function of p with the probe field near-resonant coupling $|2\rangle - |4\rangle$

Ref. [17]. For another instance, the resonant intermediate level (the singlet state) between the ground state and the two upper lying states in the atomic level configuration shown in Fig. 1 which is similar to the level scheme of the experiment mentioned in Ref. [20], and the two highest-lying states are used by a pair of mixed levels of the singlet and triplet states in sodium dimmer.

IV. Conclusion. In conclusion, we have investigated the effect of SGC on left-handedness in the four-level Y-type atom. It was found that the spontaneously generated coherence plays a significant role in the realization of left-handedness. When the SGC is weak, the atomic system doesn't display left-handedness with simultaneous negative permittivity and permeability. In the case of optimal SGC, the atomic system has a wide range for simultaneous negative permittivity and permeability, and the system is left-handedness,and the absorption is suppressed by the SGC-effect when the SGC has a large intensity. When the probe field near-resonant couples the atomic system, left-handedness appears until $p = 0.55$, and the maximum of negative refractive index is -2. We can draw from the above two cases that the strengthening of SGC produce the left-handedness. And the stronger the SGC is, the more remarkable the left-handedness appears facilely.

The work is supported by the National Natural Science Foundation of China (Grants #60768001 and 10464002).

1. U. Fano, Phys. Rev. **124**, 1866 (1961).
2. D. Agassi, Phys. Rev. A **30**, 2449 (1984).
3. J. Javanainen, Europhys. Lett. **17**, 407 (1992).
4. G. S. Agarwal, *Quantum Optics*, (Ed. by G. Höhler) Springer Tracts in Modern Physics (Springer, Berlin) V. 70, 1974.
5. S. Y. Zhu, C. F. Chan, and C. P. Lee, Phys. Rev. A **52**, 710 (1995).
6. M. Xiao, Y. Q. Li, S. Z. Jin, and J. Gea-Banacloche, Phys. Rev. Lett. **74**, 666 (1995).
7. X. G. Wei, J. H. Wu, G. X. Sun et al., Phys. Rev. A **72**, 023806 (2005).
8. M. Fleischhauer, A. Imamoglu, and J. P. Marangos, Rev. Mod. Phys. **77**, 633 (2005).
9. R. Y. Chang, W. C. Fang, Z. S. He et al., Phys. Rev. A **76**, 053420 (2007).
10. Y. Zhao, C. K. Wu, B. S. Ham et al., Phys. Rev. Lett. **79**, 641 (1997).
11. S. E. Harris, Phys. Rev. Lett. **62** 1033 (1989); A. S. Zibrov, M. D. Lukin, D. E. Nokonov et al., Phys. Rev. Lett. **75**, 1499 (1995).
12. S. Y. Zhu, and M. O. Scully, Phys. Rev. Lett. **76** 388 (1996).
13. E. Paspalakis, N. J. Kylstra, and P. L. Knight, Phys. Rev. Lett. **82**, 2079 (1999); Phys. Rev. A **61**, 045802 (2000).
14. J. H. Wu, J. Y. Gao, J. H. Xu et al., Phys. Rev. Lett. **95**, 057401 (2005).
15. J. H. Li, J. B. Liu, A. X. Chen, and C. C. Qi, Phys. Rev. A **74**, 033816 (2006).
16. O. C. H. Raymond, Phys. Rev. A **75**, 043818 (2007).
17. A. J. Li, X. L. Song, X. G. Wei et al., Phys. Rev. A **77**, 053806 (2008).
18. C. L. Wang, Z. H. Kang, S. C. Tian et al., Phys. Rev. A **79**, 043810 (2009).
19. S. I. Schmid and J. Evers, Phys. Rev. A **81**, 063805 (2010).
20. H. R. Xia, C. Y. Ye, and S. Y. Zhu, Phys. Rev. Lett. **77**, 1032 (1996).
21. A. S. Zibrov, M. D. Lukin, L. Hollberg et al., Phys. Rev. Lett. **76**, 3935 (1996).
22. T. Hong, C. Cramer, W. Nagourney, and E. N. Fortson, Phys. Rev. Lett. **94**, 050801 (2005).
23. P. Zhou and S. Swain, J. Opt. Soc. Am. B **12**, 2593 (1998).
24. A. Joshi and M. Xiao, Eur. Phys. J. D **35**, 547 (2005).

25. C. H. Bennett and D. P. Divincenzo, Nature (London) **404**, 247 (2000); M. Paternostro, M. S. Kim, and P. L. Knight, Phys. Rev. A. **71**, 022311 (2005).
26. Z. Ficek and S. Swain, Phys. Rev. A **69**, 023401 (2004).
27. J. H. Li, J. B. Liu, A. X. Chen, and C. C. Qi, Phys. Rev. A **74**, 033816 (2006).
28. X. M.Hu and J. S. Peng, J. Phys. B **33**, 921 (2000).
29. J. H. Wu, A. J. Li, Y. Ding et al., Phys. Rev. A **72**, 023802 (2005).
30. A. J. Li, J. Y. Gao, J. H. Wu, and L. Wang, J. Phys. B **38**, 3815 (2005).
31. M. V. Gurudev Dutt et al., Phys. Rev. Lett. **94**, 227403 (2005).
32. S. Dutta and K. R. Dastidar, J. Phys. B: At. Mol. Opt. Phys. **43**, 215503 (2010).
33. N. Ba, J. W. Gao, W. Fan et al., Opt. Commus. **281**, 5566 (2008).
34. V. G. Veselago, Sov. Phys.-Usp **10**, 509 (1968).
35. P. R. Berman, Phys. Rev. E **66**, 067603 (2002).
36. M. W. Feise, P. J. Bevelacqua, and J. B. Schneider, Phys. Rev. B **66**, 035113 (2002).
37. K. Aydin, I. Bulu, and E. Ozbay, Appl. Phys. Lett. **90**, 254102 (2007).
38. R. A. Shelby and D. R. Smith, Science **292**, 77 (2001).
39. J. B. Pendry, A. J. Holden, W. J. Stewart, and I. Youngs, Phys. Rev. Lett. **76**, 4773 (1996).
40. M. S. Wheeler, J. S. Aitchison, and M. Mojahedi, Phys. Rev. B **72**, 193103 (2005).
41. E. Cubukcu, Nature **423**, 604 (2003).
42. Q. Thommen and P. Mandel, Opt. Lett. **31**, 1803 (2006).
43. J. B. Pendry, Science **306**, 1353 (2004).
44. J. Käastel, M. Fleischhauer, S. F. Yelin, and R. L. Walsworth, Phys. Rev. Lett. **99**, 073602 (2007).
45. Q. Thommen and P. Mandel P, Phys. Rev. Lett. **96**, 053601 (2006).
46. M. Ö. Oktel and Ö. E. Mütecaplgu, Phys. Rev. A **70**, 053806 (2004).
47. J. Koastel, M. Fleischhauer, and R. L. Walsworth, Phys. Rev. A **79**, 063818 (2009).
48. X. M. Su, H. X. Kang, J. Kou et al., Phys. Rev. A **80**, 023805 (2009).
49. E. Paspalakis, S. Q. Gong, and P. L. Knight, Opt. Commun. **152**, 293 (1998).
50. J. H. Wu and J. Y. Gao, Phys. Rev. A **65**, 063807 (2002); J. H. Wu and J. Y. Gao, ibid. **66**, 063812 (2002).
51. J. H. Wu, Z. L. Yu, and J. Y. Gao, Opt. Commun. **211**, 257 (2002).
52. J. D. Jackson, *Classical Electrodynamics (3rd)*, N.Y.: John Wiley & Sons, 2001, Chap. 4, p. 159–162.
53. D. M. Cook, *The Theory of the Electromagnetic Field*, New Jersey: Prentice-Hall, Inc., 1975, Chap. 11.